JOURNAL OF PHYSICS AND CHEMISTRY OF SOLIDS

AN INTERNATIONAL JOURNAL

VOLUME 59 Nos. 10–12 ISSN 0022–3697

1998 OCTOBER–DECEMBER

SNS 1997

SPECIAL ISSUE

Spectroscopies in Novel Superconductors

GUEST EDITORS

A. BANSIL, R. MARKIEWICZ, S. SRIDHAR, D. LIEBENBERG

PERGAMON

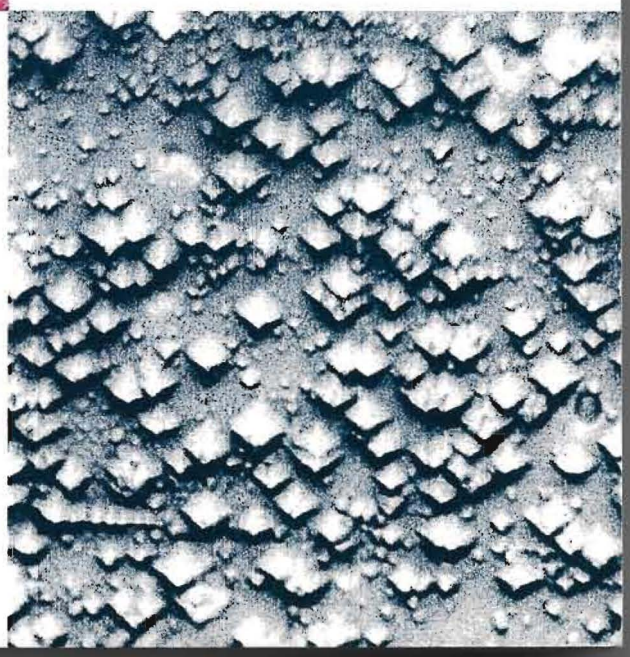

Pergamon

PII: S0022-3697(98)00121-8

J. Phys. Chem Solids Vol 59, No. 10–12, pp. 1831–1834, 1998
0022-3697/98/$ - see front matter

MICROSCOPIC THEORY OF THE LOCAL DYNAMICS IN 2-1-4 HIGH-T_C SUPERCONDUCTORS

M. D. KAPLAN[a,b,*] and G. O. ZIMMERMAN[a]

[a]Physics Department, Boston University, 590 Commonwealth Ave., Boston, MA 02215, USA
[b]Chemistry Department, Simmons College, 300 The Fenway, Boston, MA 02115, USA

Abstract—The local Jahn–Teller dynamics of the CuO_6 octahedra are explored using the conventional Jahn–Teller effect approach. The vibronic interaction of the symmetrized and hybridized electronic states with the doubly degenerate vibrations leads to four local minima of monoclinic symmetry. These results are in agreement with experimental neutron scattering data. While the obtained local minima and their combinations could be used to represent the overall crystal structure, they are different from the previously calculated free-energy minima of the crystal. © 1998 Elsevier Science Ltd. All rights reserved

Keywords: D. superconductivity, local dynamics, Jahn–Teller effects

Several investigations have centered on the microscopic theory of structural phase transitions in the 2-1-4 high-T_c superconductors [1–7]. The investigations, based on the cooperative pseudo-Jahn–Teller effect theory taking into account experimental data and symmetry group analysis, answered the following questions: (1) what is the symmetry and structure of local distortions around the Cu ion, and how they are connected to the "tilting"-mode and other crystal lattice modes; (2) how does the soft "tilting"-mode affect the electronic states; (3) how are the electronic states involved in the mechanism of the structural transitions?

Very important experimental data about the the local structure of the systems under consideration have become available [8]. Using the pair distribution function data obtained in the experiments on neutron powder diffraction for $La_{2-x}Ba_xCuO_4$, Billinge et al. [8] showed that in contrast to the predictions of the crystal structure models, the CuO_6 octahedra do not change their tilt direction in different crystal phases. The long-range structure of the high temperature phases can be considered as linear superpositions of the [110]-direction tilts. (The [110] designation may change depending on the authors' choice of the principal axes.)

We show below that the experimental data are in agreement with the earlier developed microscopic theory. Our numerical calculations confirm that the local adiabatic CuO_6 potential does have four minima phenomenologically suggested in Ref. [8]. The symmetry of each of the minima is monoclinic, however, the increase in the temperature leads to the tunneling averaging between nearest-neighbor minima [at the phase transition from low temperature tetragonal (LTT) phase to the low temperature orthorhombic (LTO) phase] and then between all four minima [at the phase transition from the LTO phase to the high temperature tetragonal (HTT) phase]. The long range structures are the combinations of these averaged local distortions.

The crystal Hamiltonian considered earlier [5–7] can be written as:

$$\hat{H} = \hat{H}_{\text{str}} + \hat{H}_{\text{ph}} + \hat{H}_{\text{el}-\text{ph}} + \hat{H}_{\text{crystal}} \tag{1}$$

where the first term describes the elastic energy of the crystal strained in the structurally ordered phase and the electron–strain interaction, H_{ph} is the phonon energy, and the next two terms are the electron–phonon interaction and the crystal field energy splitting.

Because we are interested in the local dynamics of the CuO_6 octahedra, we will initially ignore the crystal phonon dispersion, and in terms of the electron–vibration interaction, we will deal with the local distortions Q_m instead of using the creation and annihilation phonon operators. With this approach, the second and third terms are:

$$\hat{H}^m_{2,3} = \frac{1}{2}\kappa_E(Q^{m2}_{E_x} + Q^{m2}_{E_y}) + V(E^m_x Q^m_{E_x} + E^m_y Q^m_{E_y}) + G_1\sigma^m_z(Q^{m2}_{E_x} - Q^{m2}_{E_y}) + G_2\sigma^m_x Q^m_{E_x} Q^m_{E_y} \tag{2}$$

where the first term is the elastic energy of the CuO_6 cluster, and the last three terms correspond to the linear and quadratic electron–vibration interaction, κ_E is the elastic constant of the $E_g(D_{4h})$ distortions, V, G_1 and G_2 are the linear and quadratic vibronic constants. The electronic operators $E^m_{x,y}$, σ^m_z and σ^m_x are represented by the matrices:

$$E_x = \begin{pmatrix} 0 & 0 & 1 & 0 \\ 0 & 0 & 0 & 0 \\ 1 & 0 & 0 & 0 \\ 0 & 0 & 0 & 0 \end{pmatrix}; E_y = \begin{pmatrix} 0 & 0 & 0 & 0 \\ 0 & 0 & 1 & 0 \\ 0 & 1 & 0 & 0 \\ 0 & 0 & 0 & 0 \end{pmatrix} \tag{3}$$

*Corresponding author.

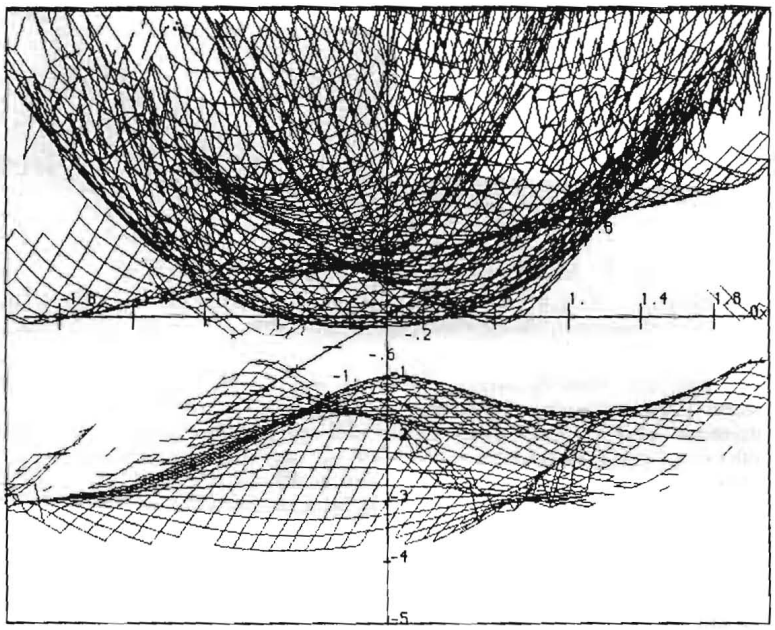

Fig. 1. Perspective view of the four lowest adiabatic potentials as a function of Q_x and Q_y with $\kappa_E = 3$, $G_1 = 0.5$, $G_2 = 1.5$, $V = 3$, $\Delta = 1$ and $\Delta_1 = 0.5$.

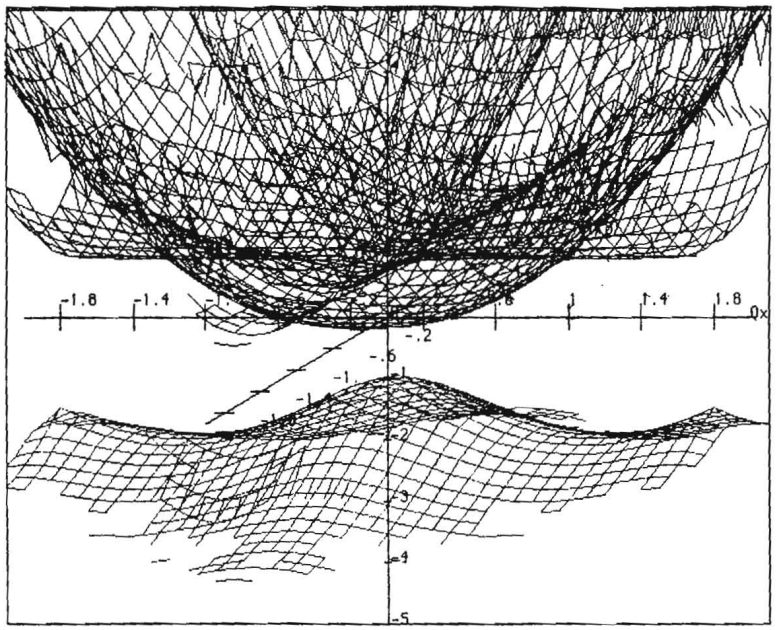

Fig. 2. Perspective view of the four lowest adiabatic potentials as a function of Q_x and Q_y with $\kappa_E = 3$, $G_1 = 1.5$, $G_2 = 0.5$, $V = 3$, $\Delta = 1$ and $\Delta_1 = 0.5$. Note the 45° rotation of the minima with respect to Fig. 1.

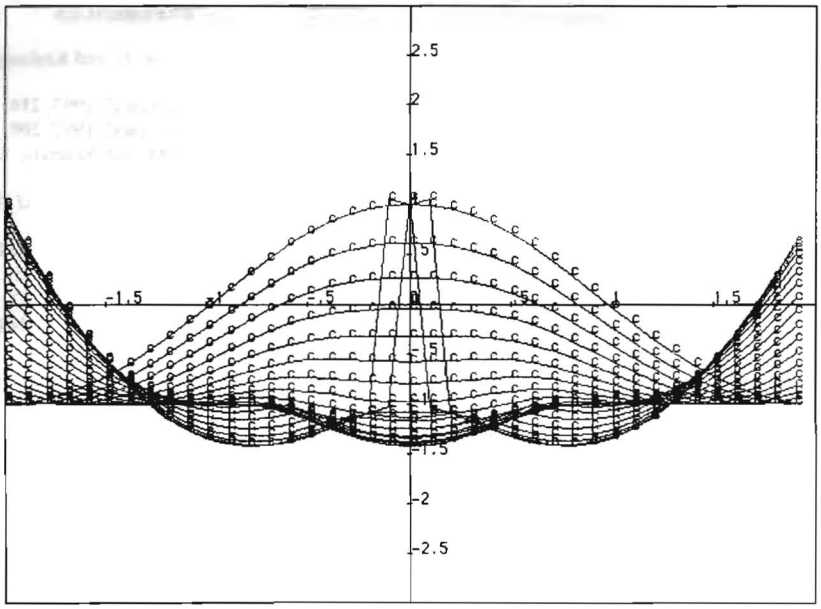

Fig. 3. View along the Q_y-axis of the first excited adiabatic potential with $\kappa_E = 3$, $G_1 = 0.5$, $G_2 = 1.5$, $V = 3$, $\Delta = 1$ and $\Delta_1 = 0.5$.

$$\sigma_x = \begin{pmatrix} 0 & 1 & 0 & 0 \\ 1 & 0 & 0 & 0 \\ 0 & 0 & 0 & 0 \\ 0 & 0 & 0 & 0 \end{pmatrix}; \quad \sigma_z = \begin{pmatrix} 1 & 0 & 0 & 0 \\ 0 & -1 & 0 & 0 \\ 0 & 0 & 0 & 0 \\ 0 & 0 & 0 & 0 \end{pmatrix}$$

The Hamiltonian (2) and operators (3) are written as a set of electronic functions

$$\Psi_1 \equiv \Psi_{B_{1g}},\ \Psi_2 \equiv \Psi_{A_{1g}},\ \Psi_{3,4} \equiv \Psi_{E_g}^{x,y} \tag{4}$$

where the ground $\Psi_{B_{1g}}$-state is separated by a Δ_1-gap from the first excited $\Psi_{A_{1g}}$-state, above which is the next excited state $\Psi_{E_g}^{x,y}$ separated from $\Psi_{A_{1g}}$ by a 2Δ-gap. (For

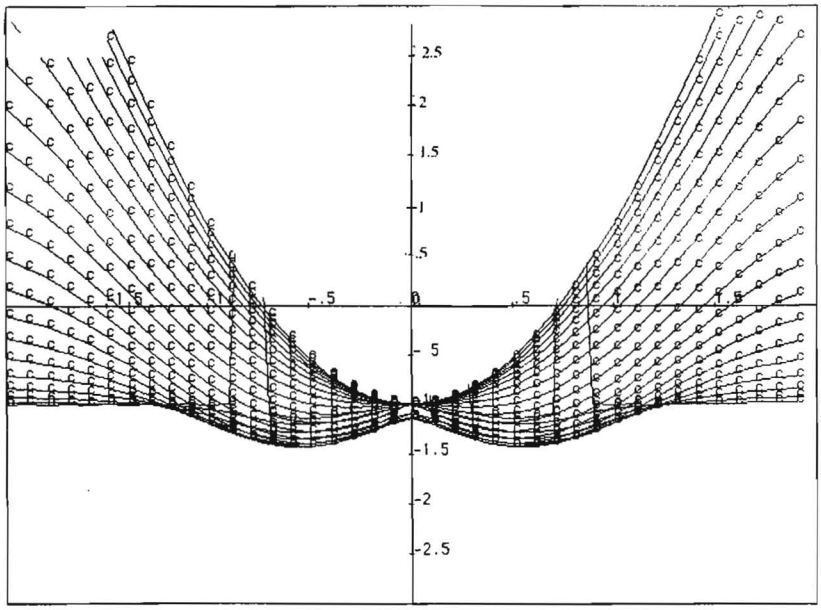

Fig. 4. View along the Q_y-axis of the first excited adiabatic potential with $\kappa_E = 3$, $G_1 = 1.5$, $G_2 = 0.5$, $V = 3$, $\Delta = 1$ and $\Delta_1 = 0.5$.

simplicity, we ignore here the $\Psi_{B_{2g}}$-excited state between $\Psi_{A_{1g}}$ and Ψ_{E_g} because the results and conclusions are virtually unchanged by this omission. This can be confirmed qualitatively and quantitatively by direct calculations.)

Samples of the calculations are shown in Figs 1–4 which show the adiabatic potentials. The value of the parameters was chosen so as to illustrate the existence of the four minima in the adiabatic potential, although those parameters will have to be adjusted to describe a real crystal. These figures clearly support our conclusions.

REFERENCES

1. Pickett, W. E., Cohen, R. E. and Krakauer, H., *Phys. Rev. Lett.*, 1991, **67**, 228.
2. Markiewicz, R. S., *Physica C*, 1993, **210**, 235.
3. Markiewicz, R. S., *Physica C*, 1992, **200**, 65.
4. Flach, S., Plakida, N. M. and Aksenov, V. L., *Int. J. Mod. Phys. B*. 1990. 4. 1955.
5. Kaplan, M. D., *Materials Theory and Modelling*, MRS, v.291, 1993, p. 223.
6. Kaplan, M. D., in *Modern Problems*, ed. A. A. Kiselev. Leningrad University, 1989, pp. 184–217.
7. Kaplan, M. D., *Physica C*, 1991, **180**, 351.
8. Billinge, S. J. L., Kwei, G. H. and Takagi, H., *Phys. Rev. Lett.*, 1994, **72**, 2282.